Int. J. Electrochem. Sci., 15 **(2020)** 1509 – 1516, doi: 10.20964/2020.02.58

International Journal of
ELECTROCHEMICAL
SCIENCE
www.electrochemsci.org

Short Communication

Simple Preparation of a Flexible CuS_x@TiO_2 Composite Electrode by Electrophoresis with Excellent Lithium Storage Performance

Jiaming Liu[1], *Yanhua Lu*[1], *Zhifeng Xu*[1], *Ruixiang Wang*[1,*], *Xue Li*[2,*]

[1] School of Metallurgy Engineering, Jiangxi University of Science and Technology, Ganzhou 341000, PR China
[2] National and Local Joint Engineering Laboratory for Lithium-ion Batteries and Materials Preparation Technology, Key Laboratory of Advanced Battery Materials of Yunnan Province, Faculty of Metallurgical and Energy Engineering, Kunming University of Science and Technology, Kunming 650093, PR China
[*]E-mail: wrx9022@163.com, 438616074@qq.com

Received: 6 October 2019 / *Accepted:* 11 December 2019 / *Published:* 31 December 2019

An anatase-type one-dimensional TiO_2 nanowire was successfully prepared by a hydrothermal method, on this basis, a flexible, uniform CuS_x@TiO_2 composite electrode was prepared by electrophoresis combined with vulcanization at high temperature. The successful loading of CuS_x particles on the TiO_2 nanowires was verified by X-ray diffraction, scanning electron microscopy and energy-dispersive X-ray spectroscopy analyses. The electrochemical tests show that the prepared flexible CuS_x@TiO_2 composite electrode has good electrochemical performance. The coulombic efficiency can be maintained above 98% at a high current density of 400 mA g^{-1}. After 80 cycles, the reversible capacity can still reach 380.1 mAh g^{-1}. The excellent electrochemical performance stems from a synergistic lithium storage process between the CuS_x and TiO_2, which not only improves the specific capacity of the material, but also effectively alleviates the volume expansion of CuS_x during the storage of lithium, thus prolonging the cycle life of the battery.

Keywords: TiO_2 nanowires, lithium ion batteries, film electrodes, composite material

1. INTRODUCTION

With the insufficient supply of petroleum energy, the development of new-tep primary batteries and secondary batteries has received widespread attention[1-9]. Lithium/sodium-ion batteries have been widely used due to their high energy density, long cycle life without memory effect, especially in electric vehicles and portable digital products[10-16]. Anode materials are one of the key factors affecting the performance of lithium-ion batteries. It is well known that graphite is used for

commercial applications, but it still faces the challenges of safety and rapid charging. The low discharge potential of the graphite anode may lead to the decomposition of an organic electrolyte and the appearance of lithium dendrites, causing a series of serious accidents[17]. In addition, anode materials with high specific capacity such as alloys, oxides and sulfides, exhibit serious volume expansion and shrinkage during lithium ion intercalation/deintercalation, and the materials are prone to undergo structural fracture and pulverization; the material eventually falls off the current collector and affects the electrochemical performance of the battery[18]. Therefore, it is very important to find a new, highly safe lithium-ion battery anode material with a large specific capacity to promote the development of lithium-ion batteries.

TiO_2 is a widely used and ideal anode material for lithium ion batteries. It has received much attention in the past ten years. Its high discharge platform (>1.5 V, vs. Li^+/Li.) protects the organic electrolyte from decomposition and prevents the formation of lithium dendrites[19-21]. At the same time, the highly stable crystal structure of TiO_2 during lithium ion intercalation/deintercalation ensures its long cycle performance [22]. Although the TiO_2 electrode has good cycling stability with high safety, the bulk anatase TiO_2 applied to the battery usually has a low practical capacity of approximately 168 mAh g^{-1}, which is much lower than the theoretical capacity of TiO_2 (335 mAh g^{-1}) [23, 24]. In addition, TiO_2 is inherently poor in ion and electron transport capabilities[25]. Therefore, many researchers have carried out a series of research work on the above issues including: (1) designing TiO_2 with 1D nanostructures to shorten the diffusion path of lithium ions, (2) mixing TiO_2 with other active substances to increase the specific capacity, and (3) coating carbon with TiO_2 to enhance the electrical conductivity of the material [26-28]. All of the above modification methods have achieved certain effects, but it is urgent to combine various modification methods to obtain a better performance.

In this work, we designed and prepared 1D TiO_2 nanowires (TiO_2-NWs) and successfully loaded CuS_x particles on them by electrophoresis with vulcanization at high temperature. Finally, a flexible CuS_x@TiO_2 electrode electrode with a special structure was obtained. The flexible CuS_x@TiO_2 electrode exhibits a better cycle performance than that of the TiO_2 electrode. The coulombic efficiency can be maintained above 98% at a high current density of 400 mA g^{-1}. After 80 cycles, the reversible capacity can still reach 380.1 mAh g^{-1}. We believe that the excellent properties of this new composite material are derived from the synergistic effect between the CuS_x and TiO_2 porous network structure.

2. EXPERIMENTAL SECTION

2.1 Preparation of the TiO_2-NWs flexible electrode

A flexible TiO_2-NWs electrode was prepared using a typical hydrothermal procedure in this work, and the method used in this article follows that described in our published articles [29, 30].

2.2 Preparation of the $CuS_x@TiO_2$ flexible electrode

The conversion of the flexible TiO_2-NWs electrode into a flexible $CuS_x@TiO_2$ electrode is as follows: 0.06 g of copper powder at 10-30 nm was added into 50 mL acetone solution under ultrasonic dispersion for 30 min. The prepared TiO_2 film and a metal Pt sheet, which were used as the working electrode and counter electrode, respectively, were soaked in the above solution. After 30 sec of an electrophoresis process at of 100 V, a flexible $Cu@TiO_2$ electrode was obtained. The as-prepared flexible $Cu@TiO_2$ electrode was further annealed with excess sulfur powder at 400 °C for 4 h with a ramp rate of 3 °C min^{-1} under a flow of argon gas, and then the flexible $CuS_x@TiO_2$ electrode was obtained.

2.3 Characterization

Structural characterization was characterized by employing a Rigaku MiniFlex II X-ray diffractometer with a Cu Kα radiation sources. The morphologies and structures of the samples were examined via scanning electron microscopy (SEM, HITACHI S-4800). Energy dispersive spectra (EDS) of the area were obtained using an energy dispersive X-ray device (HITACHI S-4800 SEM).

2.4 Characterization of electrochemical performance

The flexible electrodes were directly used as working electrodes for electrochemical characterization in CR2016 coin cells with a Celgard 2400 microporous polypropylene membrane as the separator. Lithium foils were used as the counter and reference electrodes and the electrolyte was 1 M $LiPF_6$ in a 1:1:1 (V: V: V) mixture of EC, DMC and DEC. Galvanostatic charge and discharge tests were performed with a cycle tester from a Land battery measurement system (Wuhan, China) with a cut-off voltage window of 1.0-3 V *vs.* Li^+/Li. Cyclic voltammetry (CV) curves were recorded on a CHI 660d electrochemical workstation at a scan rate of 0.1 mV s^{-1} with the same voltage window.

3. RESULTS AND DISCUSSION

Fig. 1 is an XRD pattern of the prepared flexible electrode. It can be seen that anatase TiO_2 was prepared by the hydrothermal method, and metal Cu was successfully deposited by electrophoresis, after the metal Cu was vulcanized, a copper sulfide compound was formed. Comparing the intensity of the characteristic peaks, it can be seen that after the electrophoretic deposition of the nano-Cu powder, the diffraction peak of Cu can be observed, and the diffraction peaks of the Ti foil and the TiO_2 are weakened due to the coverage of Cu particles. After a secondary calcination, the bulk diffraction peak of $Cu_{1.81}S$ was observed at $2\theta=33.2°$ and 63.5°, and the diffraction peak of Cu_2S was not detected. This can prove that the $CuS_x@TiO_2$ film cannot be successfully prepared after the secondary calcination.

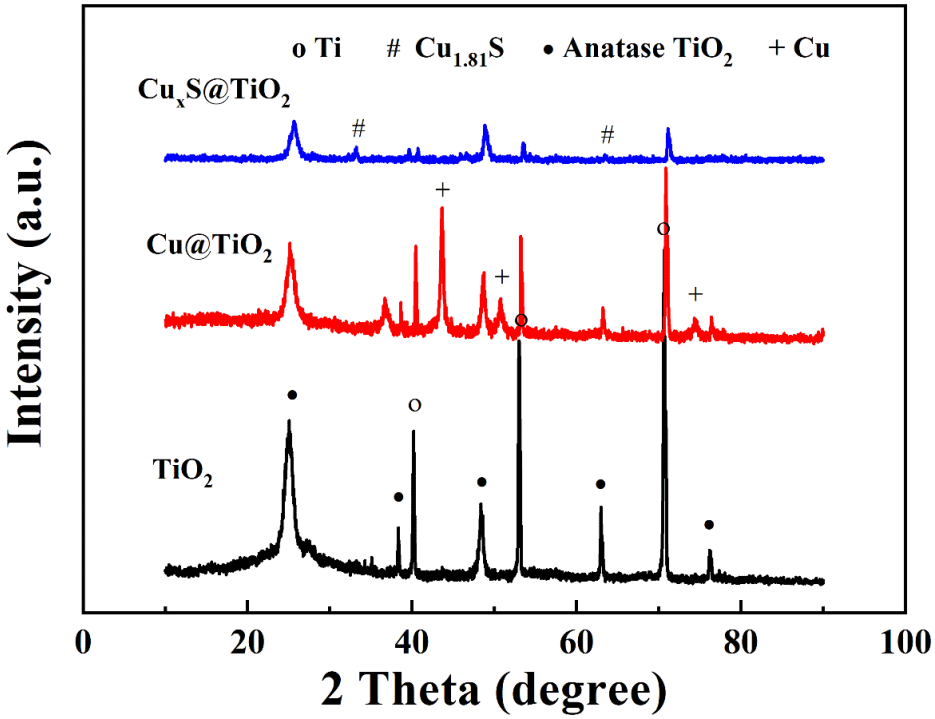

Figure 1. XRD patterns of TiO_2-NWs, Cu@ TiO_2 and $Cu_xS@TiO_2$.

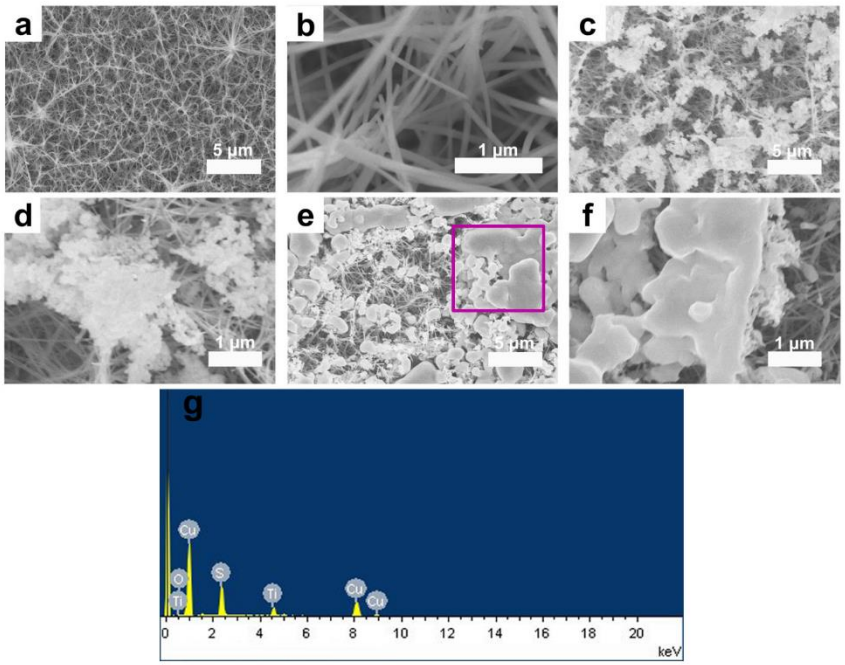

Figure 2. SEM images of (a, b) the as-prepared TiO_2-NWs, (c, d) Cu@ TiO_2, and (e, f) $Cu_xS@TiO_2$, and (g) EDX spectra of the $Cu_xS@TiO_2$ in the selected area (purple rectangle in (e)).

Fig. 2 shows SEM images of TiO_2-NWs, $Cu@TiO_2$ and $Cu_xS@TiO_2$. It can be seen that a large number of disordered TiO_2 nanowires prepared by the hydrothermal method compose a 3D network structure. The diameter of the nanowires is 60 ~ 70 nm, and the length can reach several micrometres. In Fig. 2c and d, after deposition of the nano-Cu powder by electrophoresis, the surface of the one-

dimensional TiO_2 nanowires was successfully loaded with nano-sized Cu particles. After vulcanization, the morphology did not change substantially, and the morphology of the particles enriched on the TiO_2 nanowires was still maintained (Fig. 2e, f). The EDS results (Table 1) show that the presence of the Cu and S elements can be successfully detected in the flexible electrode. The atomic ratio of Cu/S in the material is 1.97, which indicates that nano-Cu can react with S powder to form a CuS_x compound at high temperature under an inert atmosphere. Thus, a CuS_x@TiO_2 thin film electrode material was prepared.

Table 1. Elemental contents (in weight and atomic percent) of Cu_xS@TiO_2 obtained via EDX measurements.

Element	weight percent(wt%)	atomic percent (%)
O	2.36	7.34
S	18.01	27.93
Ti	9.39	9.75
Cu	70.24	54.98

Fig. 3 shows the CV curves for the first five cycles of the CuS_x@TiO_2 material with a scan rate of 0.1 mv s^{-1} and a voltage range of 1.0-3.0 V vs. Li^+/Li. It can be seen from the CV curves of Fig. 3a that the CuS_x@TiO_2 mainly has two pairs of redox peaks, A1/A2 and B1/B2, in the voltage range of 1.0~3.0V. The intercalation and delithiation reaction of A1/A2 is: $2CuS + 2Li^+ + 2e^- \rightarrow Li_2S + 2Cu_2S$, and the intercalation and delithiation reaction of B1/B2 is: $Cu_2S + 2Li^+ + 2e^- \rightarrow Li_2S + 2Cu$ [31, 32]. The two lithium intercalation reactions are the intercalation and delithiation reaction of CuS, while the intercalation and delithiation reaction of TiO_2 is not obvious. With an increased number of cycles, the A1 and B1 oxidation peaks gradually shift to 2.39 and 1.93 V, respectively, and the A2 and B2 reduction peaks shift to 2.07 and 1.56 V, respectively. Fig. 3b shows that the oxidation peak at 2.36 V gradually shifts to a low potential with an increasing number of scans until it completely disappears, indicating that a stable SEI film is gradually formed [33]. The CV results also show that the charge and discharge capacity of the material can be greatly improved after the CuS_x is attached to the surface of the TiO_2 nanowire.

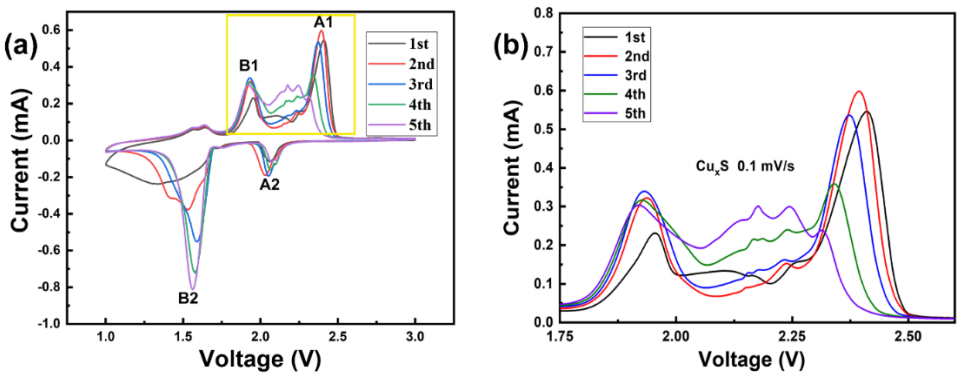

Figure 3. (a) The initial five CV curves of CuS_x@TiO_2 and (b) partial enlargement of oxidation peaks with a scanning rate of 0.1 mv s^{-1}.

Fig. 4 shows the charge-discharge cycle performance and coulombic efficiency curves of the TiO_2 and CuS_x@TiO_2 thin film electrodes at a high current density of 400 mA g^{-1}. The first discharge specific capacity and coulombic efficiency of TiO_2 are 324.5 mAh g^{-1} and 81.2%, respectively, while the initial discharge specific capacity and coulombic efficiency of CuS_x@TiO_2 after CuS_x loading reaches as high as 464.2 mAh g^{-1} and 91.6%, respectively.

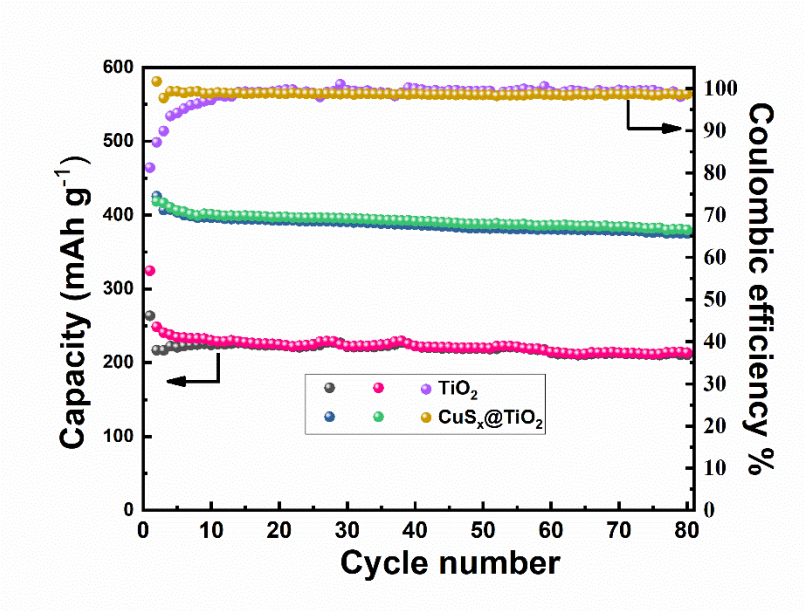

Figure 4. Cycling stability of TiO_2 and CuS_x@TiO_2 at 400 mA g^{-1}.

Table 2. Comparison of the results in this study with the reported performance of other TiO_2 and CuS_x electrode materials used as LIB anodes.

Sample	Cycling stability	Reference
Cu_xS@TiO_2	380.1 mAh g^{-1} at 400 mA g^{-1} (80 cycles)	Present work
Hydrogen modified TiO_2	225.6 mAh g^{-1} at 200 mA g^{-1} (200 cycles)	[34]
Ag@TiO_2	231.6 mAh g^{-1} at 200 mA g^{-1} (120 cycles)	[29]
SnO_2@TiO_2	834 mAh g^{-1} at 200 mA g^{-1} (100 cycles)	[35]
MoS_2@TiO_2	361.5 mAh g^{-1} at 800 mA g^{-1} (300 cycles)	[36]
Cu_2S	313 mAh g^{-1} at 100 mA g^{-1} (100 cycles)	[37]
CuS	472 mAh g^{-1} at 100 mA g^{-1} (100 cycles)	[37]

During the subsequent cycle, the coulombic efficiencies of both electrodes gradually increase to 98% and remain stable. After 80 cycles, the reversible capacities of TiO_2 and CuS_x@TiO_2 are 210.5 and 380.1 mAh g^{-1}, respectively. After the CuS_x particles are loaded, the specific capacity of the flexible electrode is significantly improved, and the capacity attenuation is reduced. Such excellent electrochemical cycle performance can be attributed to two points: 1) the high theoretical capacity of CuS_x can increase the overall reversible capacity of the composites and 2) the TiO_2 network structure increases the active area of the electrode in contact with the electrolyte and provides a good support matrix for maintaining structural integrity. It has a certain elasticity, which can effectively alleviate the

volume expansion of CuS_x during lithium storage, resulting in the extended cycle life of the electrodes [31]. The cycling stability characteristics of the TiO_2 and CuS_x electrodes are summarized in Table 2, which also compares them with the cycling stability characteristics previously reported for other TiO_2 and CuS_x electrodes used as anodes in lithium-ion battery systems.

4. CONCLUSIONS

In this work, a CuS_x@TiO_2 thin film electrode was successfully prepared by a hydrothermal method combined with electrophoresis and vulcanization. When used as an anode electrode, the flexible CuS_x@TiO_2 electrode exhibits a better reversible capacity and good cycling performance compared with those of the pure TiO_2. After 80 cycles at a high current density of 400 mA g^{-1}, the reversible capacity can still reach 380.1 mAh g^{-1} with a small capacity attenuation. The composite material has excellent electrochemical properties due to the synergistic effect between the CuS_x and the TiO_2 porous network structure. This study shows that the combination of a TiO_2 film electrode and a metal sulfide can effectively improve the specific capacity of the material and obtain excellent electrochemical performance. The as-prepared electrode is expected to be used as a replacement for carbon anodes in high performance lithium-ion batteries.

ACKNOWLEDGMENTS
The project was supported by Science and Technology Program of Education Department of Jiangxi Province in China (No. GJJ180464) and Scientific Research Foundation of JiangXi University of Science and Technology (jxxjbs17057), National Natural Science Foundation of China (Nos. 51564021, 51604132, 21965017), Key R&D Programs of Science and Technology Project of Ganzhou City ([2018] 50), Science and Technology Project of Ganzhou City ([2017] 179).

References

1. Z. L. Deng, Q. F. Yi, G. Li, Y. Chen, X. K. Yang and H. D. Nie, *Electrochim. Acta*, 279(2018)1.
2. J. T. Ding, S. Ji, H. Wang, H. J. Gai, F. S. Liu, B. G. Pollet and R. F. Wang, *Chem. Commun.*, 55(2019)2924.
3. Z. Tao, Q. F. Yi, Y. Y. Zhang, Z. L. Deng, M. Lei and X. L. Zhou, Chem. *J. Chin. Univ.*, 38(2017)101.
4. Y. Y. Zhang, Q. F. Yi, G. K. K. Zuo, T. Zou, X. P. Liu and X. L. Zhou, *J. Electrochem.*, 24(2018) 270.
5. Z. L. Deng, Q. F. Yi, Y. Y. Zhang and H. D. Nie, *J. Electroanal. Chem.*, 803(2017), 95.
6. Q. F. Yi and Q. H. Chen, *Electrochim. Acta,* 182(2015)96.
7. Q. F. Yi, Y. H. Zhang, X. P. Liu and Y. H. Yang, *Sci. Chin. Chem.*, 57(2014) 739.
8. L. Yu, Q. F. Yi, X. K. Yang and G. Li., *Chemistryselect.*, 3 (2018)12603.
9. H. L. Peng, Z. Y. Mo, S. J. Liao, H. G. Liang, L. J. Yang, F. Luo, H. Y. Song, Y. L. Zhong and B. Q. Zhang, *Sci. Rep.*, 3(2013) 1765.
10. H. S. Song, A. P. Tang, G. R. Xu, L. H. Liu, M. J. Yin and Y. J. Pan, *Int. J. Electrochem. Sci.*, 13(2018)4720.
11. H. S. Song, A. P. Tang, G. R. Xu, L. H. Liu, Y. J. Pan and M. J. Yin, *Int. J. Electrochem. Sci.*, 13(2018)6708.

12. A. P. Tang, Q. W. Zhong, G. R. Xu, H. S. Song, *Rsc Adv.*, 6(2016) 84439.
13. H. Shang, Z. C. Zuo, L. Li, F. Wang, H. B. Liu, Y. J. Li and Y. L. Li, *Angew. Chem. Int. Ed.*, 57(2018)774.
14. S. B. Xia, F. S. Li, F. X. Chen and H. Guo, *J. Alloys Compd.*, 731(2018)428.
15. J. M. Liu, D. Wang, P. Dong, J. B. Zhao, Q. Meng, Y. J. Zhang and X. Li, *Int. J. Electrochem. Sci.*, 12(2017)3741.
16. J. M. Liu, R. X. Wang, X. C. Zhong, K. Yan, Y. H. Li and Z. F. Xu, *Int. J. Electrochem. Sci.* 14(2019) 1725.
17. X. Y. Li, Y. M. Chen, L. M. Zhou, Y. W. Mai and H. T. Huang, *J. Mater. Chem. A*, 2(2014)3875.
18. S. H. Liu, Z. Y. Wang, C. Yu, H. B. Wu, G. Wang, Q. Dong, J. S. Qiu, A. Eychmueller and X. W. Lou, *Adv. Mater.*, 25(2013)3462.
19. Y. S. Hu, L. Kienle, Y. G. Guo and J. Maier, *Adv. Mater.*, 18(2006)1421.
20. D. H. Wang, D. W. Choi, J. Li, Z. G. Yang, Z. M. Nie, R. Kou, D. H. Hu, C. M. Wang, L. V. Saraf, J. G. Zhang, I. A. Aksay and J. Liu, *ACS Nano*, 3(2009)907.
21. X. Zhang, P. S. Kumar, V. Aravindan, H. H. Liu, J. Sundaramurthy, S. G. Mhaisalkar, H. M. Duong, S. Ramakrishna and S. Madhavi, *J. Phys. Chem. C*, 116(2012)14780.
22. W. Li, F. Wang, Y. P. Liu, J. X. Wang, J. P. Yang, L. J. Zhang, A. A. Elzatahry, D. Al-Dahyan, Y. Y. Xia and D. Y. Zhao, *Nano Lett.*, 15(2015)2186.
23. R. V. D. Krol, A. Goossens and J. Schoonman, *J. Phys. Chem. B*, 103(1999) 7151.
24. P. Kubiak, J. Geserick, N. Hüsing and A. Wohfahrt-Mehrens, *J. Power Sources*, 175(2008)510.
25. X. Yan, Y. J. Li, F. Du, K. Zhu, Y. Q. Zhang, A. Y. Su, G. Chen, and Y. J. Wei, *Nanoscale*, 6(2014)4108.
26. S. W. Kim, T. H. Han, J. Kim, H. Gwon, H. S. Moon, S. W. Kang, S. O. Kim and K. Kang, *Acs Nano*, 3(2009)1085.
27. F. X. Wu, Z. X. Wang, X. H. Li and H. J. Guo, *J. Mater. Chem.*, 21(2011)12675.
28. Y. M. Li, Z. G. Wang, X-J. Lv, *J. Mater. Chem. A*, 2(2014)15473.
29. H. C. Lin, X. Li, X. Y. He and J. B. Zhao, *Electrochim. Acta*, 173(2015)242.
30. J. Y. Liao, B. X. Lei, H. Y. Chen, D. B. Kuang and C. Y. Su, *Energy Environ. Sci.*, 5(2012)5750.
31. A. M. Qin, J. Y. Ji, R. Du, N. Tian, L. Liao, K. Y. Zhang and C. Wei, *Compos. Commun.*, 7(2018)47.
32. Y. R. Wang, X. W. Zhang, P. Chen, H. T. Liao and S. Q. Cheng, *Electrochim. Acta*, 80(2012)264.
33. H. C. Tao, X. L. Yang, L. L. Zhang and N. B. Ni, *J. Phys. Chem. Solids*, 75(2014)1205.
34. X. Li，J. B. Zhao，S. G. Sun，L. Huang，Z. P. Qiu，P. Dong and Y. J. Zhang, *Electrochim. Acta*, 211 (2016)395.
35. X. Li, Z. Y. Zhu, G. P. Nayaka, J. G. Duan, D. Wang, P. Dong, L. Huang, J. B. Zhao, S. G. Sun, X. H. Yu and Y. J. Zhang, *J. Alloys Compd.*, 752(2018)68.
36. Y. J. Zhang, S. B. Zhao, X. Y. Zeng, J. Xiao, P. Dong, J. B. Zhao, S. G. Sun, L. Huang and X. Li, *J. Mater. Sci.-Mater. Electron.*, 28(2017) 9519.
37. X. Li，X. Y. He，C. M. Shi，B. Liu，Y. Y. Zhang，S. Q. Wu and J. B. Zhao, *Chemsuschem*，7(2014) 3328.